Electronic Supplementary Material (ESI) for Nanoscale.

Supporting Information

Gap-enhanced optical bistability in plasmonic core - nonlinear shell dimers

Artyom Movsisyan, and Henrik Parsamyan*

Institute of Physics, Yerevan State University, A. Manoogian 1, Yerevan, 0025, Armenia

*Corresponding author: *hparsamyan@ysu.am*

I. INFLUENCE OF THE SHELL THICKNESS

The analysis of the influence of the shell thickness on the optical response of the C-Sh dimer is shown in Figure S1. Here, we carried out numerical simulations by considering shell thickness of 2 nm and 8 nm and compared the results to the main model with a 5 nm shell. The schematic sketch is depicted in Supporting Information Figure S1 (a), while (b-d) show the spectra of (b) the intensity enhancement at the nanogap centre, (c) scattering efficiency and (d) extinction efficiency for the considered values of the shell thickness. The inset in (b) shows an enlarged view of the intensity enhancement maxima. Analysis of the optical response of the C-Sh dimer shows that the intensity enhancement, which mainly defines the optical bistable response of the plasmonic-core Kerr-shell dimer, practically is not affected by shell thickness variations around 5 nm as long as the nanogap space is filled by the Kerr medium. For instance, the maximum intensity enhancement values for systems with 2 nm, 5 nm and 8 nm shells are about 3.1×10^4, 3.2×10^4 and 3.5×10^4, respectively. It is seen that the scattering and absorption efficiencies also vary slightly as the shell thickens. Hence, one can expect a similar range of input intensities to observe optical bistability for C-Sh dimers with different shell thicknesses, meaning that the bistable response will not be noticeably affected due to shell thickness variations. Further decrease in the shell thickness below 1.5 nm (half of the inter-core gap) will result in a sharp drop of the intensity inside the shell since the system will be composed of two separate C-Sh particles[1].

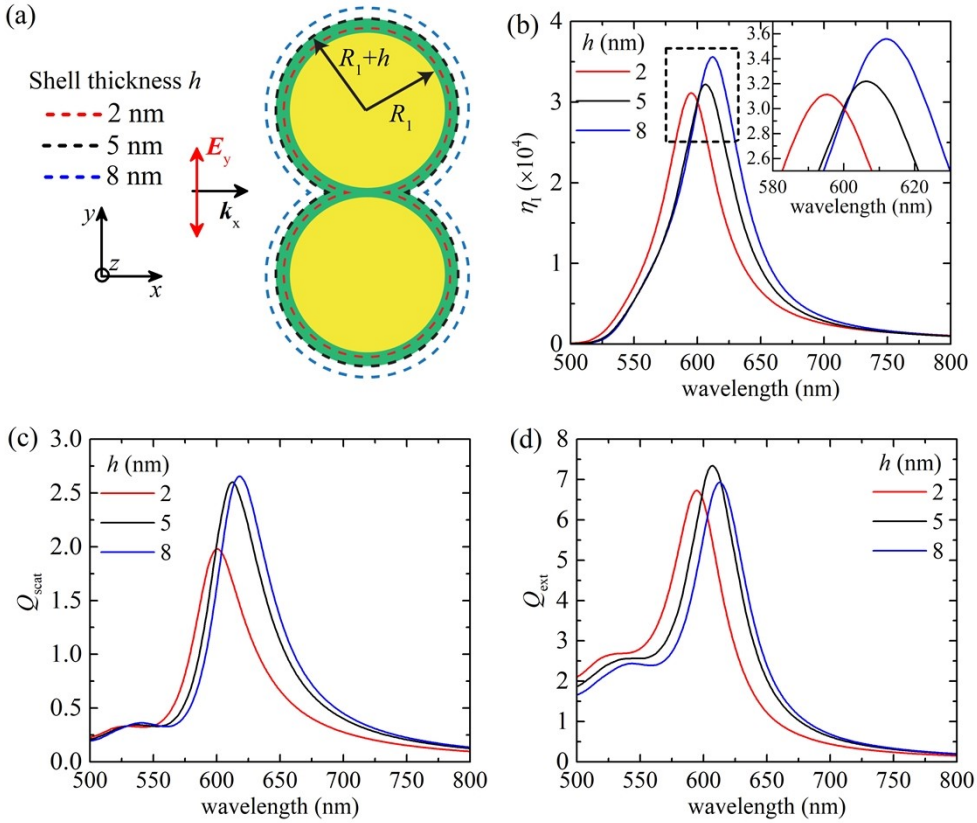

Figure S1. The influence of the shell thickness on the optical response of the C-Sh dimer. (a) Schematic of the C-Sh dimer with tree shell thickness indicated by dashed lines: 2 nm (red), 5 nm (black) and 8 nm (blue). (b-d) Spectra of (b) the intensity enhancement at the nanogap centre, (c) scattering efficiency and (d) extinction efficiency for the considered values of the shell thickness. The inset in (b) shows the enlarged view of the intensity enhancement maxima.

As an extreme case, we considered a configuration with a 1 nm shell and 3 nm gap. Such a system will represent two separate C-Sh particles with a surface-to-surface distance of 1 nm and the interparticle region being air. The schematic of the system is illustrated in Figure S2(a). Figure S2 (b) shows the spectra of scattering, absorption, and extinction efficiencies, while Figure S2 (c) depicts the intensity enhancements at the nanogap centre and in the shell at points A and B, respectively. In such a configuration the coupling between plasmonic cores is noticeably weakened resulting in a decrease in the intensity inside the shell, which, in turn, will reduce the nonlinear response. The resonant value of the intensity enhancement at point A is about 2.57×10^4, whereas

that at point B is 0.58×10^4. Such a sharp drop in the shell intensity will require noticeably higher driving fields to observe bistable behaviour. In addition, the enhancement will be strongly affected by the possible surface-to-surface distance changes as the mutual shell is absent in this case.

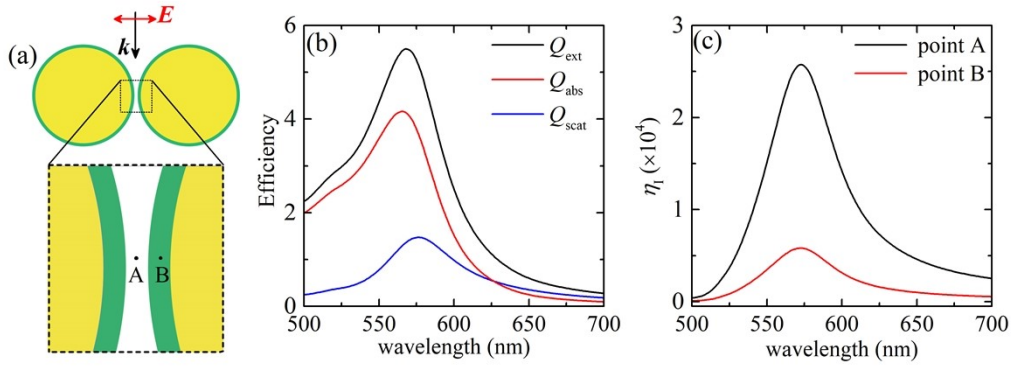

Figure S2. Optical response of the C-Sh dimer with the shell thickness of 1 nm and surface-to-surface distance between cores of 3 nm. (a) Schematic illustration of the dimer with the shell thickness of 1 nm and the zoomed view of the interparticle region. A and B are the points where intensity enhancements for the interparticle region and the shell were evaluated. (b) Extinction (black), absorption (red) and scattering (blue) efficiency spectra for the C-Sh dimer. Comparison of intensity enhancement spectra at the nanogap centre (black curve, point A) and shell (red curve, point B).

II. POLARIZATION-DEPENDENCE OF THE OPTICAL RESPONSE

Polarization dependence of the optical response of the C-Sh dimer is depicted in Figure S3, where (a-c) show spectra of (a) scattering and (b) extinction efficiencies and (c) intensity enhancement at the nanogap centre for polarization angle values of 0° (black lines, polarization parallel to the dimer axis), 45° (red lines) and 90° (blue lines, polarization perpendicular to the dimer axis). It is seen that at φ = 90°, the dimer cores are decoupled enhancing the incident intensity only by an order. Figure S3 (d) shows the intensity enhancement as a function of the polarization angle φ (black solid line). The incidence wavelength is 605 nm. Symbols stand for the fitting by a function proportional to $\cos^2(\varphi)$. The inset shows the enlarged view in the range from 0° to 15°. In the case of small orientation mismatch of the dimer axis in respect to the incident field polarization only the electric field component parallel to the dimer axis will contribute to the intensity enhancement, and the latter will scale as $\cos^2(\varphi)$, where φ is the angle between the dimer axis and driving field polarization[2]. Taking into account that $\cos^2(\varphi)$ is a slowly varying function for small arguments, small changes in the dimer axis with respect to the incident field polarization up to 10° practically will not affect the intensity enhancement in the nanogap area. This is also confirmed by results presented in Figure S3(d). Particularly, the intensity enhancement at the nanogap centre changes from $I(\varphi = 0°) = 3.26\times10^4$ to $I(\varphi = 10°) = 3.16\times10^4$. Taking into account these values, one can estimate the range of input intensities of the optical bistability for φ = 10° by simply scaling those for φ = 0° (225-375 kW/cm^2) proportional to the ratio of intensity enhancements. For instance, given that $I(\varphi = 0°)/I(\varphi = 10°) \sim 1.032$, the range of input intensities of the optical bistability for φ = 10° is estimated to be approximately 230-390 kW/cm^2.

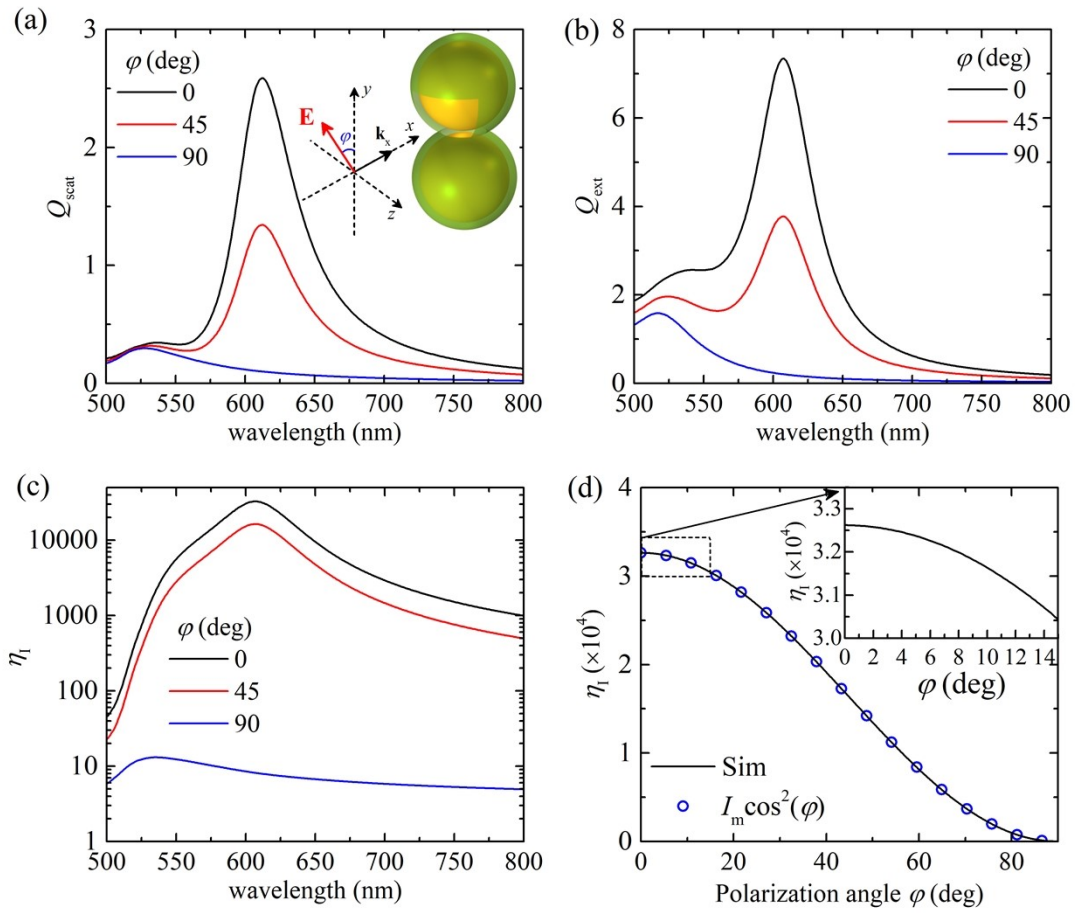

Figure S3. Polarization dependence of the optical response of the C-Sh dimer. (a-c) Spectra of (a) scattering efficiency, (b) extinction efficiency and (c) intensity enhancement at the nanogap centre for polarization angle values of 0° (black lines, polarization parallel to the dimer axis), 45° (red lines) and 90° (blue lines). The inset in (a) depicts the schematic of the C-Sh dimer and incident field orientation. (d) Intensity enhancement at the nanogap centre as a function of the polarization angle φ (black solid line) at the incidence wavelength of 605 nm. Symbols stand for the fitting by a function proportional to $\cos^2(\varphi)$. The inset shows the enlarged view in the range from 0° to 15°.

III. LINEAR OPTICAL RESPONSE OF THE DIMER WITH SILVER CORES

Figure S4 shows the linear optical response of the Ag-core nonlinear shell dimer. The complex dielectric function of Ag is taken from the experimental data[3].

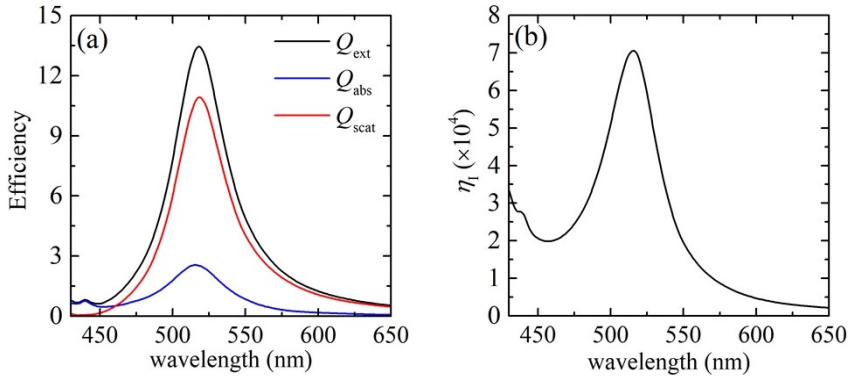

Figure S4. Linear optical response of the considered dimer with Ag cores. Spectra of (a) extinction (black), scattering (red) and absorption (blue) efficiencies under a plane wave polarized along the dimer axis. (b) Intensity enhancement spectrum at the nanogap centre.

It is seen that the resonance appears around 517 nm with an extinction efficiency of around 13, which is mainly contributed by scattering. The intensity enhancement factor at the nanogap centre reaches up to 7×10^4. This value is almost twice as high as that for the dimer with Au cores, meaning that the optical bistability in the dimer with Ag cores can be achieved at lower driving intensities.

References

1 I. O. Osorio-Román, A. R. Guerrero, P. Albella and R. F. Aroca, *Anal. Chem.*, 2014, **86**, 10246–10251.

2 M. Gittinger, K. Höflich, V. Smirnov, H. Kollmann, C. Lienau and M. Silies, *Nanophotonics*, 2020, **9**, 401–412.

3 P. B. Johnson and R. W. Christy, *Phys. Rev. B*, 1972, **6**, 4370–4379.